

## Tunable Single-Pair Hollow-Beam-Converter Dark-Field Microscopy

This content has been downloaded from IOPscience. Please scroll down to see the full text.

2013 Jpn. J. Appl. Phys. 52 100202

(<http://iopscience.iop.org/1347-4065/52/10R/100202>)

View [the table of contents for this issue](#), or go to the [journal homepage](#) for more

Download details:

IP Address: 140.113.38.11

This content was downloaded on 24/04/2014 at 14:15

Please note that [terms and conditions apply](#).

## Tunable Single-Pair Hollow-Beam-Converter Dark-Field Microscopy

Che-Liang Tsai<sup>1</sup>, Long Hsu<sup>2\*</sup>, Kuang-Lung Huang<sup>3</sup>, and Ken-Yuh Hsu<sup>1</sup>

<sup>1</sup>Department of Photonics and Institute of Electro-Optical Engineering, National Chiao Tung University, Hsinchu 300, Taiwan

<sup>2</sup>Department of Electrophysics, National Chiao Tung University, Hsinchu 300, Taiwan

<sup>3</sup>Department of Electro-Optical and Energy Engineering, Mingdao University, Peetow, Changhua 524, Taiwan

E-mail: long@cc.nctu.edu.tw

Received March 28, 2013; accepted July 29, 2013; published online September 10, 2013

A tunable single-pair hollow-beam-converter (TSHBC) dark-field microscopy is proposed and fabricated. The TSHBC is composed of one pair of parallel reflective mirrors of complementary cone shape. By simply adjusting the longitudinal separation between the two mirrors of TSHBC, a dark-field image with more high contrast and high energy efficiency can be obtained for a given objective lens. Furthermore, the selection criteria of the condenser lens and objective lens are provided for the structure of an optimal dark-field microscopy with TSHBC.

© 2013 The Japan Society of Applied Physics

The bright-field microscope is a popular optical instrument for viewing a magnified image of a specimen. However, as a specimen is transparent or its refractive index is close to that of the surroundings, light scattering from the specimen is reduced and the imaging becomes weak. Furthermore, the unscattered illuminating light forms a background noise that reduces the contrast of the image. Under this situation, using a bright-field microscope to view a specimen becomes difficult. Instead, dark-field microscopy is an effective solution to resolve this problem.<sup>1–3)</sup>

The idea of contrast enhancement in traditional dark-field microscopy lies in the fact that the central portion of the illumination beam, which is the primary source of the background level, is blocked. Therefore, the signal-to-noise ratio in a dark-field image is higher than that in a bright-field image, the image contrast in the dark field is thus improved. In practice, the central portion of the illumination beam is blocked simply by inserting a small disc as a stopper in front of the condenser lens. Nevertheless, the price of high energy loss has been paid, since most of the illuminating light is blocked by the stopper.<sup>4–7)</sup>

To resolve the issue of high energy loss in traditional dark-field microscopy, a new structure of a hollow-beam-converter is fabricated in this study and proposed in this paper. This structure is derived from a tunable two-pair hollow-beam-converter that was used in a semiconductor process previously reported.<sup>8)</sup> The structure consists of two pairs of conical reflective mirrors. The first pair of the mirrors shifts the central part of the incident beam to its peripheral to generate a hollow beam. Then, the second pair is used to adjust the size of the hollow beam. In this study, we simplify the tunable two-pair hollow-beam-converter structure into a tunable single-pair hollow-beam-converter (TSHBC) and use it in the dark-field microscopy applications. In this TSHBC structure, the full light intensity of the incident beam is used to illuminate the specimen. Therefore, it will generate the higher signal intensity without introducing background noise, and the issue of high-energy loss in traditional dark-field microscopy can be resolved.

In this setup, we only need to adjust the Longitudinal Separation (LS),  $d$ , between the conical mirrors of the pair, and the inner and outer radii of the hollow beam can be varied. Then, by deploying a condenser lens to focus the hollow beam, the oblique angles of the focused beam can be turned accordingly. The oblique angles of the beam illuminating the specimen determine the effective numerical

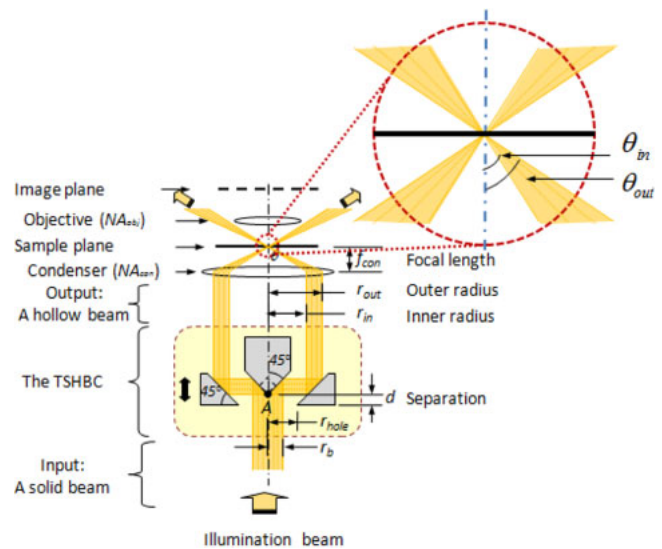


Fig. 1. (Color online) Schematic diagram of a dark-field microscopic unit with the TSHBC.

aperture of the condenser lens. By turning  $d$  so as the effective numerical aperture to match the condenser lens as well as the objective lens, dark-field microscopy with a high image contrast can be accomplished.

Figure 1 illustrates a dark-field microscopic unit with the TSHBC. The TSHBC consists of one pair of parallel mirrors of complementary cone shape arranged as a coaxial structure centered on the optical axis of the unit. The incline angles of both cones are set at  $45^\circ$  with respect to the optical axis of the TSHBC. The LS ( $d$ ) between the two conical reflectors is adjustable. An important feature here is that adjusting  $d$  will induce changes in the inner and outer radii of the incident beam, yet it will not affect the optical alignment of the system.

As shown in Fig. 1, a collimated illumination beam is converted by the TSHBC into a hollow beam with inner and outer radii, respectively, which are found to be

$$r_{in}(d) = r_{hole} + d, \quad (1a)$$

$$r_{out}(d) = r_{hole} + d + r_b, \quad (1b)$$

where  $r_b$  is the radius of the incident beam,  $r_{hole}$  is the radius of the open hole of the concave cone mirror, and  $d$  is the distance between the conical reflectors. Equations (1a) and (1b) show that the inner and outer radii of the hollow beam

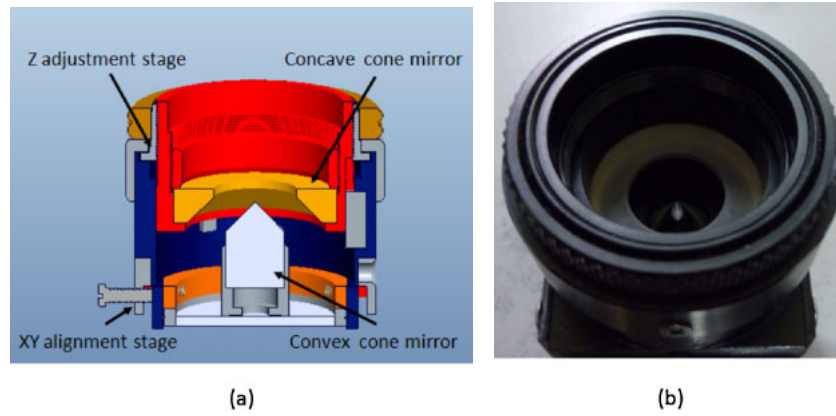


Fig. 2. (Color online) (a) Optomechanical assembly schematic and (b) photo of real TSHBC.

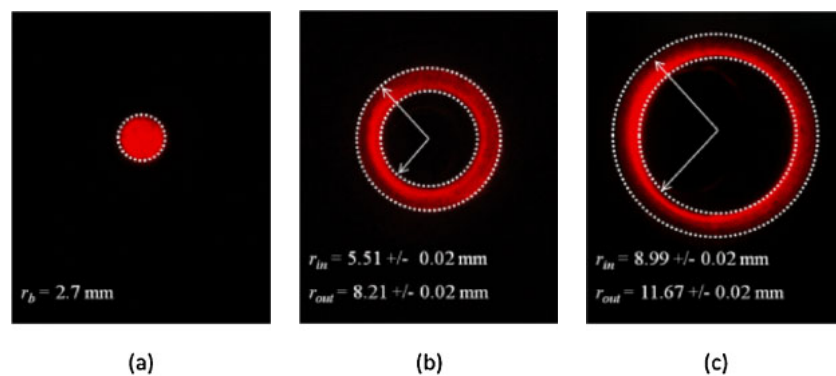


Fig. 3. (Color online) Cross-sectional views of (a) a collimated laser beam into the TSHBC, (b) the hollow beam emerging from the TSHBC at  $d = 0.50$  mm, and (c) the hollow beam at  $d = 4.00$  mm.

can be adjusted simply by turning the parameter  $d$ . Note that in order for the TSHBC to collect the entire illumination beam,  $r_{\text{hole}}$  must be larger than  $r_b$ . Here, it is fixed at 5.0 mm.

Figure 1 shows that the hollow beam is followed by a condenser lens with the focal length  $f_{\text{con}}$  to illuminate the specimen. The oblique angles of the illumination range from

$$\theta_{\text{in}}(d) = \tan^{-1}[r_{\text{in}}/f_{\text{con}}] = \tan^{-1}[(r_{\text{hole}} + d)/f_{\text{con}}]$$

to

$$\theta_{\text{out}}(d) = \tan^{-1}[r_{\text{out}}/f_{\text{con}}] = \tan^{-1}[(r_{\text{hole}} + d + r_b)/f_{\text{con}}].$$

If the specimen is immersed in a medium of refractive index of  $n_{\text{med}}$ , then the effective numerical aperture of the illuminating beam will range from  $n_{\text{med}} \sin \theta_{\text{in}}$  to  $n_{\text{med}} \sin \theta_{\text{out}}$ .

Therefore, in order for the condenser lens to capture the entire energy of the illuminating hollow beam, the following criterion for the condenser lens must be fulfilled:

$$NA_{\text{con}} > n_{\text{med}} \sin \theta_{\text{out}} = n_{\text{med}} \sin\{\tan^{-1}[(r_{\text{hole}} + d + r_b)/f_{\text{con}}]\}, \quad (2)$$

where  $NA_{\text{con}}$  is the numerical aperture of the condenser lens.

On the other hand, in order to keep the focused illumination beam from entering the objective lens, which will contribute to the background noise, the following criterion on the objective lens must be satisfied:

$$NA_{\text{obj}} < n_{\text{med}} \sin \theta_{\text{in}} = n_{\text{med}} \sin\{\tan^{-1}[(r_{\text{hole}} + d)/f_{\text{con}}]\}, \quad (3)$$

where  $NA_{\text{obj}}$  is the numerical aperture of the objective lens. Equations (2) and (3) provide the selection criteria for the condenser lens and objective lens, respectively. Equation (3) also indicates that, for a given objective lens, by turning  $d$ , more light scattering from the specimen can be collected by the objective lens so that the image contrast can be improved. The largest scattering signal collection and thus the optimal contrast of the dark-field image can be achieved when the following condition of the objective lens is satisfied:

$$NA_{\text{obj}} = n_{\text{med}} \sin \theta_{\text{in}}. \quad (4)$$

Figure 2(a) shows the optomechanical assembly of the TSHBC, and a photograph of the fabricated TSHBC is shown in Fig. 2(b). In the structure, the convex cone mirror is fixed on an XY alignment stage to make the two reflector mirrors coaxial. The concave cone mirror can be adjusted via a Z adjustment stage along the optical axis at 0.50 mm displacement per one rotation and the full adjustment range is 6.00 mm.

To characterize the hollow beam generated by the TSHBC, a collimated laser beam with a radius  $r_b$  of 2.70 mm was incident into the  $r_{\text{hole}}$  of 5.0 mm. Figure 3(a) shows a cross section of the solid beam. In Fig. 3(b),  $d$  was set at 0.50 mm, and  $r_{\text{in}}$  and  $r_{\text{out}}$  were measured as  $5.51 \pm 0.02$  and  $8.21 \pm 0.02$  mm, respectively. In Fig. 3(c),  $d$  was set at 4.00 mm,  $r_{\text{in}}$  and  $r_{\text{out}}$  were measured as  $8.99 \pm 0.02$  and  $11.67 \pm 0.02$  mm. Here, the beam radii are statistically determined at which light intensity drops to  $e^{-2}$  of its peak intensity.

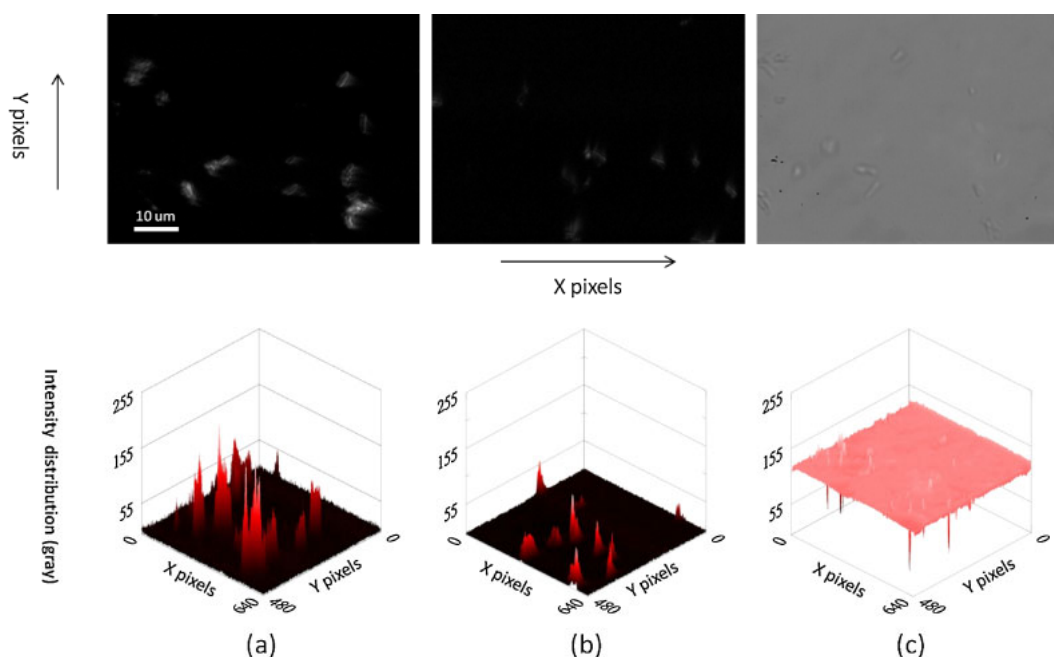


**Fig. 4.** (Color online) Dark-field images of *E. coli* cells and their intensity profiles at (a)  $d = 0.00$  and (b)  $4.00$  mm, respectively. (c) Conventional bright-field image of *E. coli* cells and its intensity profile.

According to Eqs. (1a) and (1b), for  $d = 0.50$  mm,  $r_{in}$  and  $r_{out}$  are calculated to be  $5.50$  and  $8.20$  mm, respectively. And for  $d = 4.00$  mm,  $r_{in}$  and  $r_{out}$  equaled  $9.00$  and  $11.70$  mm, respectively. The designed values and the measured data fit to each other within an error of  $0.3\%$ .

The TSHBC was assembled with an oil-immersed condenser lens with  $NA_{con} = 1.28$  and  $f_{con} = 4.17$  mm, and a  $60\times$  objective lens with  $NA_{obj} = 0.85$  to form a dark-field microscope. The beam focused by the condenser lens illuminates a group of *E. coli* cells immersed in water with  $n_{med} = 1.33$ .

Figures 4(a) and 4(b) show the dark-field images of the *E. coli* cells and their intensity distributions at  $d = 0.00$  and  $4.00$  mm, respectively. Figure 4(c) shows a bright-field image of the *E. coli* cells and its intensity distribution. As can be seen in the figures, the background level of the dark-field images is much lower, and the contrast of the dark-field image is much sharper. Furthermore, a comparison between Figs. 4(a) and 4(b) shows that the signal level in Fig. 4(a) is higher. This result confirms, as shown by our design expressed in Eqs. (3) and (4), that a smaller  $d$  produces a better image contrast as long as Eq. (3) is satisfied. In this system,

$NA_{obj}$  of the objective lens is  $0.85$ ,  $n_{med} \sin \theta_{in}$  is  $1.02$  at  $d = 0.00$  mm, and  $n_{med} \sin \theta_{in}$  is  $1.21$  at  $d = 4.00$  mm; both of these cases satisfy Eq. (3). Thus,  $d = 0.00$  mm is the optimal value that gives a high contrast of the dark-field image.

In summary, a new TSHBC for dark-field microscopy is proposed and fabricated. A dark-field microscopy imaging with optimal contrast has been demonstrated simply by adjusting  $d$  of the TSHBC. We also illustrate the selection criteria for the condenser lens and the objective lens for accomplishing the best signal-to-noise ratio as well as the most efficient energy use in dark-field microscopy.

- 1) B. Witlin: *Science* **102** (1945) 41.
- 2) S. Matsunaga, S. Kawano, T. Higashiyama, N. Inada, and T. Kuroiwa: *Micron* **28** (1997) 185.
- 3) V. V. Senatorov: *J. Neurosci. Methods* **113** (2002) 59.
- 4) J. W. M. Chon, M. Gu, C. Bullen, and P. Mulvaney: *Opt. Lett.* **28** (2003) 1930.
- 5) J. Prikulis, F. Svedberg, M. Käll, J. Enger, K. Ramser, M. Goksör, and D. Hanstorp: *Nano Lett.* **4** (2004) 115.
- 6) C. Sönnichsen and A. P. Alivisatos: *Nano Lett.* **5** (2005) 301.
- 7) X. Liu, Y. Huang, and J. U. Kang: *J. Biomed. Opt.* **16** (2011) 046003.
- 8) Y. Ogura: Japan Patent 684760 (1994).